Statistical Theory of Quasi-Geostrophic Turbulence

JACKSON R. HERRING

National Center for Atmospheric Research,[1] Boulder, CO 80307

(Manuscript received 22 March 1979, in final form 12 December 1979)

ABSTRACT

Within the context of statistical homogeneity, we examine geostrophic turbulence, employing a simple, eddy-damped closure. We find for decaying turbulence that high wavenumbers tend toward three-dimensional isotropy, as predicted by Charney, but wavenumbers smaller than the energy peak tend toward an approximate two-dimensional state, with the crossover wavenumber near the peak energy wavenumber. The high-wavenumber energy spectrum is found to be log-modified k^{-3}, where k is the *three-dimensional* wavenumber. Analytic information for the isotropization rate at small scales as well as for the large-scale "barotropization" is proposed. Finally, we describe the relation of these results to the more familiar layered approximations of the equations of motion.

1. Introduction

In his 1971 paper on geostrophic turbulence, Charney argued that the dynamics of quasi-geostrophic flow (neglecting boundaries) lead—at small scales—to homogeneous and isotropic statistics for both the energy and temperature variance. He further produced general arguments—based on the familiar conservation laws for energy and enstrophy for inviscid flow—that the isotropic energy inertial range would be k^{-3}, where k is the *three-dimensional* wavenumber.

Charney's results at first glance appear somewhat paradoxical. Consider, for example, the case of stratified flow with spacial homogeneity. Then the equations of motion simply state that the quasi-geostrophic potential vorticity is convected in horizontal planes. The question then arises, how can these patently anisotropic dynamics result in isotropic statistics for spectra?

Some insight into this issue may be obtained if we consider homogeneous inviscid flow supported by a finite wavenumber band and ask for the absolute equilibrium statistics. If this is done, we find the usual energy spectrum $E(k) = k^2/(a + bk^2)$, where (a,b) are constants related to the total energy and (quasi-geostrophic) enstrophy (Kraichnan, 1967). Note, however, that for the present problem $\mathbf{k}$ is a three-dimensional rather than a two-dimensional vector and, consequently, $E(\mathbf{k})$ is three-dimensionally isotropic. The physical interpretation of the isotropy in this case is traceable to a tendency of the flow to equilibrate two-thirds the kinetic and one-third the potential energy. We have not touched on the stability of the three-dimensional absolute equilibrium solution.

The quasi-geostrophic equations also admit strictly two-dimensional solutions whose inviscid equipartition form is $k/(a + bk^2)$. These solutions are an extreme form of anisotropy, and purely thermodynamic reasoning rules them out since their entropy is smaller than the three-dimensional case. Also, such strictly two-dimensional solutions are unstable to three-dimensional perturbations, as has already been demonstrated by Jacobs and Wiin-Nielsen (1966).

For real flows with dissipation, equipartition ideas are only suggestive, and more dynamical arguments must be advanced to treat the issue of isotropizing of quasi-geostrophic flow. In the present paper, we investigate this problem by means of the statistical theory of turbulence, employing a simplified version of the test field model (TFM) (Kraichnan, 1971) which is equivalent to the eddy-damped quasi-normal approximation (Orszag, 1974). We note incidentally that for inviscid flow the TFM satisfies an H theorem (Carnavale *et al.*, 1980), which implies that for the present problem the three-dimensional isotropic state—mentioned earlier—is monotonically approached. The entropy in this case is the logarithm of the model energy spectrum.

Our motive here is not only to examine the issue of high-wavenumber isotropy, but to discover how much of the observed dynamics of quasi-geostrophic flow can be comprehended in the context of homogeneous flow. What we observe is that both large-scale barotropization and small-scale isotropization are

[1] The National Center for Atmospheric Research is sponsored by the National Science Foundation.

0022-4928/80/050969-09$06.25

reproduced correctly by the homogeneous version of the theory. We recall that both these effects have been observed in the numerical simulations of Rhines (1977) and others [see Rhines (1979) for a summary of other work] who use vertically layered approximations to the equations of motion. Our use of the term "barotropic" here means strictly two-dimensional, rather than quasi-two-dimensional, as would be implied by near isotropy in the stretched coordinate frame. It is hoped that the present continuously stratified, statistical treatment yields insights which complement the above-cited calculations. The theory permits a calculation of rates of large-scale barotropization and small-scale isotropization.

With regard to the issue of the isotropization of homogeneous flow, our results are complex. Thus, as noted above, solutions to initial value problems typically show a development of a barotropic region at scales larger than the peak energy wavenumber, a baroclinic range of scales near the energy peak, followed by an inertial range at progressively smaller scales. The inertial range does become more isotropic as k increases, but only very gradually (approximately logarithmically).

The resulting flow may be characterized roughly by saying that scales larger than the energy peak are barotropic, while scales smaller than the energy peak are three-dimensionally isotropic. For self-similar decay, the critical dividing wavenumber decreases—with the energy peak wavenumber—as time increases. In terms of our earlier thermodynamic discussion, three-dimensional isotropy is achieved by the passing of this critical wavenumber into the origin.

The present paper treats only statistically homogeneous flow. Here this restriction is much more limiting than in the Navier-Stokes equations, whose dynamics imply that in the absence of boundaries the flow becomes eventually three-dimensionally homogeneous even if the ensemble of initial data is not. There is nothing in the quasi-geostrophic equations which enforces vertical homogeneity, although an initially homogeneous ensemble is self-propagating. Thus, our calculation can only give insight into those initial value problems which approximate vertical homogeneity.

2. Statistical theory of quasi-geostrophic turbulence

a. Equations of motion and kinematics

As noted in the Introduction, we confine our attention here to homogeneous flows, ignoring boundaries and other complications such as topography and the beta effect. The equations of motion are

$$(\partial/\partial t + \mathbf{u}\cdot\nabla)\nabla^2\psi = 0. \tag{2.1}$$

Here, ∇^2 is the three-dimensional Laplacian [in stretched z coordinates, $z \to z(N/f)$, where f is the Coriolis parameter, N the Brunt-Väisälä frequency assumed constant here] and $\mathbf{u}$ is the horizontal velocity field, derived from the streamfunction ψ by

$$(u,v) = (-\psi_y, \psi_x) = \mathbf{u}.$$

We denote the covariance of the potential vorticity, $-\nabla^2\psi = \zeta$, by

$$\tilde{\phi}(\mathbf{x},\mathbf{x}',t) = \tilde{\phi}(\mathbf{x} - \mathbf{x}', t) \equiv \langle\zeta(\mathbf{x},t)\zeta(\mathbf{x}',t)\rangle. \tag{2.2}$$

We shall need vertical correlation lengths for a given horizontal wavenumber K. Accordingly, we introduce two- and three-dimensional transforms of $\tilde{\phi}$:

$$\phi(\mathbf{k},t) \equiv (2\pi)^{-3}\int d(\mathbf{x} - \mathbf{x}') \times \exp[i\mathbf{k}\cdot(\mathbf{x} - \mathbf{x}')]\tilde{\phi}(\mathbf{x} - \mathbf{x}', t), \tag{2.3}$$

$$\phi(\mathbf{K}|z) \equiv (2\pi)^{-2}\int \exp(i\mathbf{K}\cdot\boldsymbol{\rho})\phi(\boldsymbol{\rho},z)d\boldsymbol{\rho} = \int_{-\infty}^{\infty}\exp(-ik_z z)\phi(\mathbf{k})dk_z. \tag{2.4}$$

Here $\mathbf{x} = (\boldsymbol{\rho},z)$, $\mathbf{k} = (k_x,k_y,k_z)$, and $\mathbf{K} = (k_x,k_y)$. Our notation is such that the arguments of ϕ specify the dimensionality of the transform. Inverting (2.4) yields

$$\phi(\mathbf{k}) = (2\pi)^{-1}\int_{-\infty}^{\infty}\exp(ik_z z)\phi(\mathbf{K}|z)dz. \tag{2.5}$$

We shall, for simplicity, assume horizontal isotropy so that $\phi(\mathbf{k})$ may be written as

$$\phi(\mathbf{k}) = \phi(k,\mu) = \sum_0^\infty \phi_n(k)P_n(\mu), \tag{2.6}$$

where μ is the polar angle and P_n are Legendre functions. It is convenient to define a ϕ-based vertical (correlation) length scale L by

$$L_\phi(K,t) = \int_{-\infty}^{\infty} dz\ \phi(K|z)/\phi(K|0).$$

In terms of the angular distribution (2.6), we have

$$L_\phi(K) = (2\pi)\phi(K,0)\left[\int_{-\infty}^{\infty} dk_z\ \phi(k,\mu)\right]^{-1}. \tag{2.7}$$

If $L_\phi(K,t)$ increases with t, the flow becomes more barotropic at wavenumber K. Note that as $L_\phi \to \infty$, $\phi(k,\mu) \to \delta(\mu)$, according to (2.5).

It is also convenient to have gross measures of baroclinicity and barotropy of the flow. For this purpose, we introduce total integral scales in the vertical and horizontal:

$$L_H(\phi) \equiv \int_{-\infty}^{\infty} \langle \zeta(\mathbf{x})\zeta(\mathbf{x} + \mathbf{i}\xi)\rangle d\xi / \langle \zeta^2(\mathbf{x})\rangle$$

$$= \int_{-\infty}^{\infty} \tilde{\phi}(\mathbf{i}\xi) d\xi / \tilde{\phi}(0), \tag{2.8a}$$

$$L_V(\phi) \equiv \int_{-\infty}^{\infty} \langle \zeta(\mathbf{x})\zeta(\mathbf{x} + \mathbf{k}\xi)\rangle d\xi / \langle \zeta^2(\mathbf{x})\rangle$$

$$= \int_{-\infty}^{\infty} \tilde{\phi}(\mathbf{k}\xi) d\xi / \tilde{\phi}(0), \tag{2.8b}$$

where **i** and **k** are unit vectors in the x and z directions. Using (2.4)–(2.7)

$$\frac{L_V(\phi)}{L_H(\phi)} = \frac{\int_0^{\infty} dkk\{\phi_0(k) - (1/2)\phi_2(k) + \cdots\}}{\int_0^{\infty} dkk\{\phi_0(k) + (1/4)\phi_2(k) + \cdots\}}, \tag{2.8c}$$

where the series (2.6) is terminated at second order. We have here computed length scales pertaining to the vorticity covariance $\tilde{\phi}$, but could just as easily have computed them with respect to the streamfunction ψ and its covariance Ψ. We denoted the latter by $L_H(\Psi)$, $L_v(\Psi)$ and $L_\Psi(k)$, using (2.7) or (2.8) with $\phi \to \Psi$.

b. Statistical theory

We now introduce the expansion (2.6) into the statistical-moment equations corresponding to (2.1) and obtain equations of motion for $\phi_n(k)$. We employ here a variant of the simple quasi-normal eddy-damped theory (EQN). This simple procedure appears to capture the essential physics of the problem, while a more elaborate theory—such as the ALHDI[2] (Kraichnan and Herring, 1978)—appears prohibitively complex. Our present procedure corresponds to the TFM algorithm, in which only the isotropic parts of the relaxation rates are retained.

It is convenient to employ the total energy $U(\mathbf{k}) \equiv \phi(\mathbf{k})/k^2$ as the basic dynamical variable. This quantity is related to the kinetic energy spectrum $V(\mathbf{k})$ by

$$\langle |\mathbf{v}(\mathbf{k})|^2 \rangle \equiv V(\mathbf{k}) = \sin^2\theta\, U(\mathbf{k}), \quad \mu = \cos\theta.$$

The equations of motion for its Legendre representatives U_m [see Eq. (2.6)] are (see the Appendix for derivation)

$$\dot{U}_0 = T^k(U_0,U_0) - (1/5)[T^k(U_0,U_2) + T^k(U_2,U_0)] + \tilde{T}^k(U_2,U_2) + \cdots, \tag{2.9}$$

$$\dot{U}_2 = -T^k(U_0,U_0) + R(U_0,U_2) - (1/7)T^k(U_2,U_2) + \cdots. \tag{2.10}$$

[2] Abridged Lagrangian history direct interaction.

Here

$$T^k(U_1,U_2) = \int_\Delta dpdq\, B_{kpq}\theta_{kpq}U_2(q)[U_1(p) - U_1(k)], \tag{2.11}$$

$$\tilde{T}^k(U_2,U_2) = (1/70)\int_\Delta dpdq\, B_{kpq}\theta_{kpq}U_2(q) \times \{(1 + 9x^2)U_2(p) - (1 + 9y^2)U_2(k)\}, \tag{2.12}$$

$$R^k(U_0,U_2) = (1/14)\int_\Delta dpdq\, \theta_{kpq}U_2(q)(1 + 9y^2) \times \{(B_{kpq} + B_{kqp})U_0(p) - B_{kpq}U_0(k)\} - (5/7)\int dpdq\, B_{kpq}\theta_{kpq}U_2(k)U_0(q), \tag{2.13}$$

$$B_{kpq} = (4\pi/3)(pq/k^3)(p^2 - q^2) \times (k^2 - q^2)(1 - x^2). \tag{2.14}$$

In these expressions (x,y,z) are interior angles in triangle (k,p,q) and θ_{kpq} are the triple moment relaxation rates, for which we employ the prescription recommended by Pouquet *et al.* (1975)

$$\theta_{kpq}^{-1} \approx \left\{\int^k k'^2 dk' E(k')\right\}^{1/2} + \left\{\int_0^p p'^2 dp' E(p')\right\}^{1/2} + \left\{\int^q q'^2 dq' E(q')\right\}^{1/2}. \tag{2.15}$$

Details of the angular expansion are set out in the Appendix.

To gain some insight into these equations, we consider an initial value problem for which U_0 is the thermal equilibrium spectrum, $1/(a + bk^2)$, and $U_2 = 0$. Then $\dot{U}_0 = \dot{U}_2 = 0$, and the flow remains (three-dimensionally) isotropic. Further, if $U_2 = 0$ and U_0 is an inertial range spectrum $1/k^5$ [so that $E(k) = 2\pi k^2 U(k) \propto k^{-3}$], again, $\dot{U}_0 = \dot{U}_2 = 0$. However, if U_0 departs from either inviscid equipartition or inertial range (as it must at small k), then $\dot{U}_2 \neq 0$ and according to (2.10) has the opposite sign from $T(U_0,U_0)$. Hence at small k, where $T > 0$, the flow becomes barotropic ($\dot{L}(K) > 0$) [see Eq. (2.7)] and at larger k, where $T(U_0,U_0) \lessapprox 0$, the flow becomes more baroclinic ($\dot{L}(k) \lessapprox 0$). After U_2 has developed to a finite value, the $R^k(U_0,U_2)$ term acts to restore isotropy. This term is formally similar to the return rate in strictly two-dimensional turbulence (Herring, 1975), the last term in (2.13) acting as an eddy-damping rate. However, for strictly two-dimensional flows we may show that

$$\int_0^{\infty} dp \int_{|k-p|}^{k+p} dq B_{kpq}^{(2)} U_0(q) \geq 0,$$

with

$$B^{(2)}_{kpq} = (2/k^2)(p^2 - q^3)(k^2 - q^2)(1 - x^2)^{1/2}.$$

However, for the present problem, the counterpart to the above integral [using Eq. (2.11)] becomes negative at small k. This leads to a destabilization of the small k region and, since there the flow becomes initially barotropic, the implication is that the barotropization will proceed indefinitely unless limited by the nonlinear terms in (2.10). We shall return presently to a more thorough discussion of this point after developing some analytic approximations valid for small k.

We now give the results of some asymptotic analysis which supports these assertions. This is done by evaluating the transfer functions in (2.9)–(2.11) for k very much smaller (or larger) than the energy-containing wavenumber. For large k, we obtain

$$T^k(U_0,U_0) = (8\pi/45)\int p^4U_0(p)dpk^{-4}\partial(\theta_{kkp}k^4\partial) \times (k^2U_0(k)/\partial k)/\partial k + \cdots, \quad (2.16)$$

$$R^k(U_0,U_2) = (136/105)(\pi/21)\int p^4dpU_2(p)\theta_{kkp} \times \{\partial^2(k^2U_0(k))/\partial k^2 + (32/17)k^{-1}\partial(k^2U_0(k))/\partial k\} + \cdots - (5/7)\mu(k)U_2(k), \quad (2.17)$$

where

$$\mu(k) = \int B_{kpq}dpdq\theta_{kpq}(q)U_0(q), \quad (2.18)$$

with B_{kpq} is given by (2.14). These are asymptotic expansions in which $(p/k)^n$ is the small expansion parameter [see Pouquet *et al.* (1975) and Herring (1975) for more complete details]. They are plausible for the inertial range and the beginning of the dissipation range but inappropriate for the far dissipation range. We note that (2.16)–(2.17) are consistent with $U_0(k) \sim k^{-5}$, $U_2(k) = 0$ in that if $U_2 = 0$, $T^k(k^{-5},k^{-5}) = 0 + \cdots$. Heuristic inertial range arguments [applied to Eq. (2.16)] may further be used to establish $E(k) \approx k^{-3}[\ln(k)]^{-1/3}$, similar to results obtained for two-dimensional turbulence by Kraichnan (1971). Eq. (2.17) gives the large k return-to-isotropy behavior. The first term here gives the production of anisotropy stemming from the straining of an isotropic field, $U_0(k)$, by large-scale (rms) strain $[\int dpp^4U_2(p)]^{1/2}$. This term is zero for the inviscid equipartition solution $U_0(k) \approx k^{-2}$. The last term in (2.17) is the familiar eddy-drain term, which damps anisotropy due to the turbulent self-interaction. A more careful examination of this type of equation (see Herring, 1975) shows that the eddy-drain term is nearly canceled by positive production terms for which $(p/k) \approx 1$ and which expansion (2.17) omits. This cancellation effectively reduces the value of the eddy-drain term to the level of the eddy circulation time $(\int_0^k p^2E(p)dp)^{1/2}$.

At small k, (2.9)–(2.11) become

$$T^k(U_0,U_0) \to (32\pi/45)k^2\int_0^\infty p^2dp(U_0(p))^2\theta_{kpp} + (16\pi/45)k^2U_0(k)\int_0^\infty p^2dpU_0(p)\theta_{kpp} + \cdots, \quad (2.19)$$

$$R^k(U_0,U_2) \to (1108\pi/2205)k^2\int_0^\infty p^2dpU_2(p)U_0(p)\theta_{kpp} - (304\pi/2205)k^2U_0(k)\int_0^\infty p^2dpU_2(p)\theta_{kpp} + (80\pi/315)k^2U_2(k) \times \int_0^\infty p^2dpU_0(p)\theta_{kpp} + \cdots. \quad (2.20)$$

The first term in (2.19) leads to $E(k) \to k^4$, if the initial data have $E(k,0) = 0$, a point exploited recently by Lesieur and Schertzer (1978) in their study of the decay law for isotropic turbulence. The second term in (2.19) is a negative eddy viscosity. Its physics is somewhat different than that of two-dimensional, isotropic turbulence. In the latter case, arguments introduced by Kraichnan (1976) may be used to show that negative eddy viscosity can and does occur *only* if a low wavenumber cutoff is introduced. In the present problem, however, there is no cutoff. The return-to-isotropy term (2.20) has a similar negative eddy viscosity term, but its effect is masked by other terms in (2.20).

The above discussion of energy transfer at low wavenumber suggests that it has the elements of an instability. Thus, if (2.19) approximates the energy transfer at small k and the equation for $\dot{U}_0$ also contains an energy input, we expect $U_0(k) \to \infty$. This would not necessarily be the case for two-dimensional turbulence for which the positive eddy viscosity limits the buildup of energy at k near 0.

However, the above argument neglects the possible effects on $T^k(U_0,U_0)$ of the increasing barotropicity of the energy-containing region. Note that according to (2.19) and (2.20), $\dot{U}_2(k)$ at small k becomes negative and hence, according to (2.8), the flow tends toward two-dimensionality. Since we know that the eddy viscosity is positive for two dimensions (excluding a low wavenumber cutoff), we may conclude that this instability is quenched before the flow becomes fully barotropic. The quenching effects are, of course, contained in the higher harmonics [e.g., $T^k(U_2,U_2)$], which we have not discussed.

3. Some numerical results

To illustrate the discussion of the last section, we consider some numerical calculations of (2.9)–(2.13). We solve these equations on a wavenumber span ($0 \leq k \leq 200$) and apply a biharmonic viscous dissipation to damp out high-wavenumber enstrophy. Its form is

$$\nu(k) = \begin{cases} 0, & k \leq 150, \\ 10(k^2 - 150^2)^2/(200^2 - 150^2)^2, & k \geq 150. \end{cases} \quad (3.1)$$

Numerical experimentation showed that if (3.1) is applied to an energy spectrum, normalized to unity and with peak wavenumber near $k = 2$, then (3.1) was sufficient to prevent an appreciable damming-up of enstrophy near $k = 200$. At the same time, the dissipation is sufficiently weak so that a k^{-3} inertial range developed and extended over ($10 \leq k \leq 100$). We examine three initial value problems consisting of

$$U_0(k,0) = Ak^2/(k_0^7 + k^7) \equiv F(k), \qquad U_2(k,0) = 0, \quad (3.2a)$$

$$U_0(k,0) = F(k), \qquad U_2(k,0) = F(k), \quad (3.2b)$$

$$U_0(k,0) = F(k), \qquad U_2(k,0) = -F(k). \quad (3.2c)$$

Here, $k_0 = 2$, $A = 7k_0^2 \sin(5\pi/7)/(2\pi^2)$. At large k, Eqs. (3.2a)–(3.2c) developed smoothly into a dissipation range, while at small k—where little energy resides initially—they developed into profiles produced by dynamics, rather than as fossils of initial conditions. We note in this connection that (2.19) implies that if $U_0(k,0)$ increases less steeply than k^2, then $U_0(k,t)$ and $U_2(k,t)$ will simply retain their initial shapes for a substantial time. If, however, $U(k,0)$ increases as k^2, then the subsequent development of $U(k,t)$ is controlled by the inverse cascade and $U(k) \approx k^2$ as $k \to 0$. We examine the development of (3.2a) in some detail and present results for (3.2b) and (3.2c) only in summary form.

Fig. 1 gives the kinetic energy for spectrum (2.3a) (solid line) and twice the potential energy (dashed line) at $t = 6.0$—about six, large-scale eddy circulation times. For complete isotropy, these quantities are equal. The dotted line is the initial kinetic energy. We note that by $t = 6$, the energy spectrum has shifted significantly toward larger scales, while at the same time maintaining approximately its initial shape. At wavenumbers smaller than the peak energy wavenumber k_{max} the flow is significantly deficient in potential energy, while at k larger than k_{max} a slight excess of potential energy is observed. The precise degree of anisotropy is better observed in Fig. 2a, which gives the ratio ρ of potential to total energy:

$$\rho(k) \equiv \tfrac{1}{3}[1 + \tfrac{2}{5}U_2(k)/U_0(k)]$$

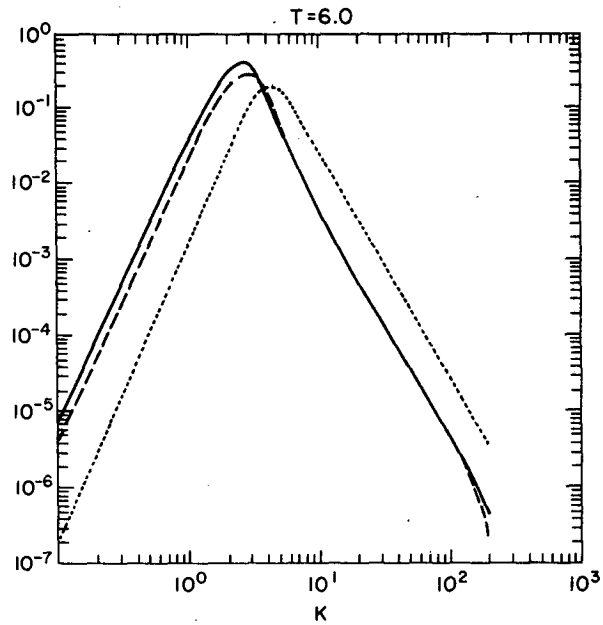

FIG. 1. Energy spectra for initial condition (3.2a). Solid line, kinetic energy at $t = 6.0$; dashed line, three halves the potential energy, $t = 6.0$; dotted line, kinetic energy at $t = 0$.

as a function of k [here the initial spectrum (3.2a) is the solid line]. Fig. 2b gives the energy transfer functions for comparison, as given by the right-hand sides of (2.9) and (2.10) [for case (3.2a) only]. Fig. 2a indicates a fairly sharp front separating the region of strong barotropic flow ($\rho < \frac{1}{3}$) from baroclinic flow ($\rho > \frac{1}{3}$). At small k ($k \leq 1.0$), the angular distribution of $U(k, t = 6)$ is essentially $\sim\sin^2\theta$, and the angular harmonic expansion (2.6) needs more terms for accuracy ($n > 2$). The region just beyond k_{max} appears most strongly baroclinic, with a very slowly decaying anisotropy throughout the inertial range. The region $k \geq 10^2$ may be viewed as the dissipation range, where the biharmonic viscosity begins to affect seriously the shape of the spectra. It is strongly barotropic but this feature is clearly dependent on our representation of dissipation as isotropic in stretched z coordinates [see Eq. (3.1)]. Here we are relying on the Reynolds-number independence of the large scales (Herring *et al.*, 1974) to argue that inertial range results are independent of details of the dissipation range, at least at large Reynolds numbers. Fig. 2b indicates that the energy back transfer region is strongly two-dimensional. The shape of $T_0(k)$ is typical of two-dimensional turbulence. Also shown in Fig. 2a are $\rho(k)$ for initial spectrum (3.2b) (the dashed line), and for (3.2c) (the dotted line). The figure suggests that all three initial spectra tend toward the same universal shape.

Fig. 3 depicts the spectral length scales $L(K)$ for streamfunction and vorticity spectra, as given by Eq. (2.7), and as normalized by the appropriate total

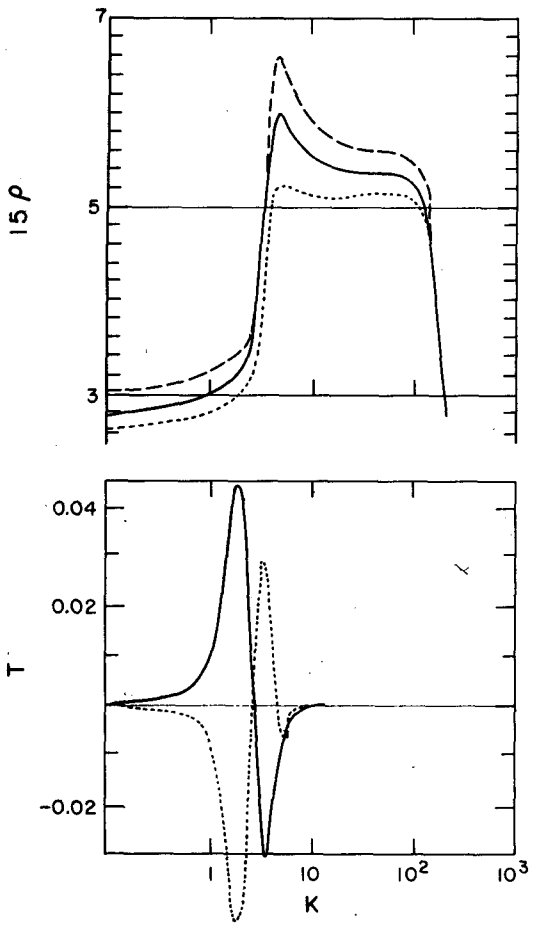

FIG. 2. Ratio of potential to kinetic energy, $\rho(k, t = 6.0)$, Eq. (2a), and total energy transfer functions at $t = 6.0$, Eq. (2b). Fig. 2a shows ρ for the three initial conditions: Eq. (3.2a), solid line; Eq. (3.2b), dashed line; and Eq. (3.2c), dotted line. Fig. 2b is for initial conditions (3.2a) only. Curves are $T(k) \equiv 2\pi k^2$ times right-hand side of (2.9) (solid line) and (2.10) (dotted line).

vertical length scale $L_V(t)$ [Eq. (2.8b)]. Shown here are only results for Eq. (3.2a). We note that the vorticity length-scale distribution shifts, self-similarly, back to smaller k, whereas the streamfunction length scale exhibits rapid growth for k smaller than k_{max}. As remarked earlier, our truncated P_n expansion ($n \leq 2$) becomes suspect at smaller k for $t \geq 6$.

Finally, Fig. 4 shows the track of $L_H(t)$, $L_V(t)$ for both streamfunction and vorticity as a function of time, with the ticks indicating time segments $dt = 0.5$. All three initial conditions [Eqs. (3.2a)–(3.2c)] are shown. The general increase of these lengths as a function of time is typical of decaying turbulence. However, we note that the vorticity trajectory remains more nearly three-dimensional (running more nearly parallel to the line $L_V = L_H$) than that for the streamfunction. The degree of two-dimensionality may be judged by the asymptotic angle of the ψ-based L_H, L_V tracks. Totally two-dimensional flow would have a vertical track, while for three-dimensional flow the ψ track would run at 45°. The asymptotic ψ tracks appear to be only slightly more obtuse than the initial conditions (3.2c) [$U(\mathbf{k}) \propto \sin^2\theta$] would indicate. Note, however, that according to Fig. 2a this flow becomes strongly three-dimensional at larger k. The ϕ-based L_H, L_V tracks appear more three-dimensional but also appear to tend toward two-dimensionality. This is clearly a result of large negative values of ρ (see Fig. 2a) at small k weighing more than the rather small positive values at larger k. Had L been computed for $\nabla^2\phi$, a more nearly 45° track would undoubtedly have been found.

A prolate spectrum such as Eq. (3.2b) represents a flow field with excessive vertical variation and, in the limit $U(k,\mu) \approx \delta(1 - \mu)$, the nonlinear interactions vanish. It therefore represents a pathological exact solution and it is of some interest to know whether the flow exhibits any tendency to seek it out. Our calculations here—as is indicated in Figs. 2a and 4b—indicate that it does not. Less severe, nonsingular, prolate initial conditions are the statistical analogue of a baroclinically unstable state. The oblate initial conditions, on the other hand, represent near two-dimensional states, and the extreme limit $U(\mathbf{k},0) \approx \delta(\mu)$ is simply two-dimensional turbulence. The stability of this singular state has not (to our knowledge) been explored via statistical theory.

The instability of the prolate initial conditions found here may be understood from an examination of Eqs. (2.9) and (2.10) without numerical integra-

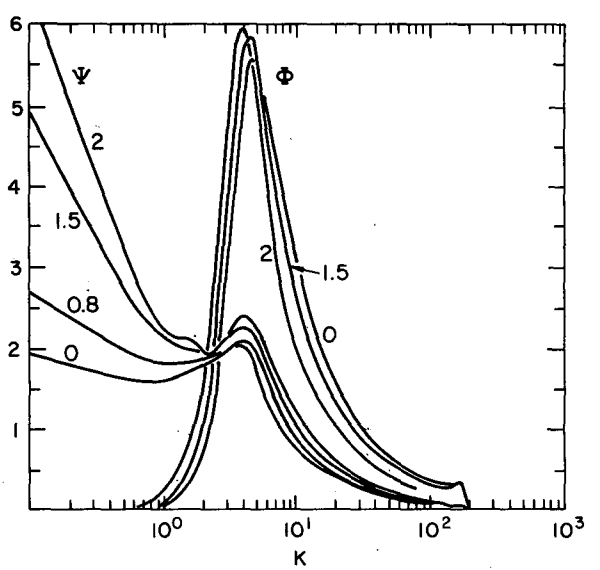

FIG. 3. Two-dimensional vertical correlation length-scale distributions, $L(K)$ [see Eq. (2.7)] for both streamfunction (Ψ) and vorticity spectra Φ. Curves are labeled by evolutions time t. Only initial spectrum (3.2a) is shown.

tion. Thus the first term on the right-hand side of (2.10) indicates that, in the inverse cascade region, $U(\mathbf{k})$ tends toward oblateness regardless of the sign of U_2, since the return-to-isotropy terms are weaker than the first term at small k. On the other hand, at large k, the return to isotropy is the larger term, since $U(\mathbf{k})$ is, or quickly becomes, inertial so that the first term nearly vanishes.

4. Concluding comments

The present calculations for homogeneous quasi-geostrophic flow show a rather clear tendency for the small scales to seek three-dimensional isotropy in the stretched coordinate frame. At the same time, the rate of isotropization is weak, characteristic of two-dimensional turbulence rather than three. This weak relaxation toward isotropy arises from the rather steep k^{-3} spectrum, for which the eddy circulation rates are nearly independent of k. Consequently, the rate of approach is no larger at small scales than at large scales. We view this tendency toward small-scale isotropy as a manifestation of the flow to seek three-dimensional equipartition. At large scales, on the contrary, the flow is strongly two-dimensional in that for initial value problems the total energy spectrum (without forcing) tends toward $\sim\sin^2\theta$, where θ is the polar angle. This qualitative tendency would be expected from a naïve consideration of the horizontal convection of geostrophic vorticity, i.e., simply stepping the homogeneous version of the equations of motion forward in time a couple of steps and ensemble averaging. The dividing wavenumber between the near-two-dimensional and near-three-dimensional flow occurs in self-similar decay near the energy peak wavenumber $k_{\max}$. The transition is rather abrupt, and scales somewhat smaller than $k_{\max}$ characteristically pick up a baroclinic character.

The present study may be compared to layered calculations, particularly the statistical treatment of a two-layered system developed by Salmon (1978), and the earlier thermal equilibrium study by Salmon *et al.* (1977). These studies differ from the present in that their subject constitutes an inhomogeneous system on the vertical wavenumber lattice $k_z = (0, \pm k_0)$, and the continuous horizontal wavenumber spectrum $\mathbf{K}$. The presence of other k_z's $< k_0$ are excluded by boundary conditions, and those $> k_0$ are discarded for computational reasons, although such a two-layer model can be realized in the laboratory. The earlier study by Salmon *et al.* concluded that, in thermodynamic equilibrium, scales larger than the Rossby radius of deformation $(f^2k_0/g')^{1/2}$ were essentially two-dimensional, whereas smaller scales were mixed barotropic-baroclinic. Perhaps these equilibrium results may be interpreted from the present perspective by saying that the flow has become as nearly three-dimensionally isotropic as the geometrical constraints and modal representation would allow. Thus the only way of representing vertical correlations larger than the Rossby radius is to have the flow completely two dimensional.

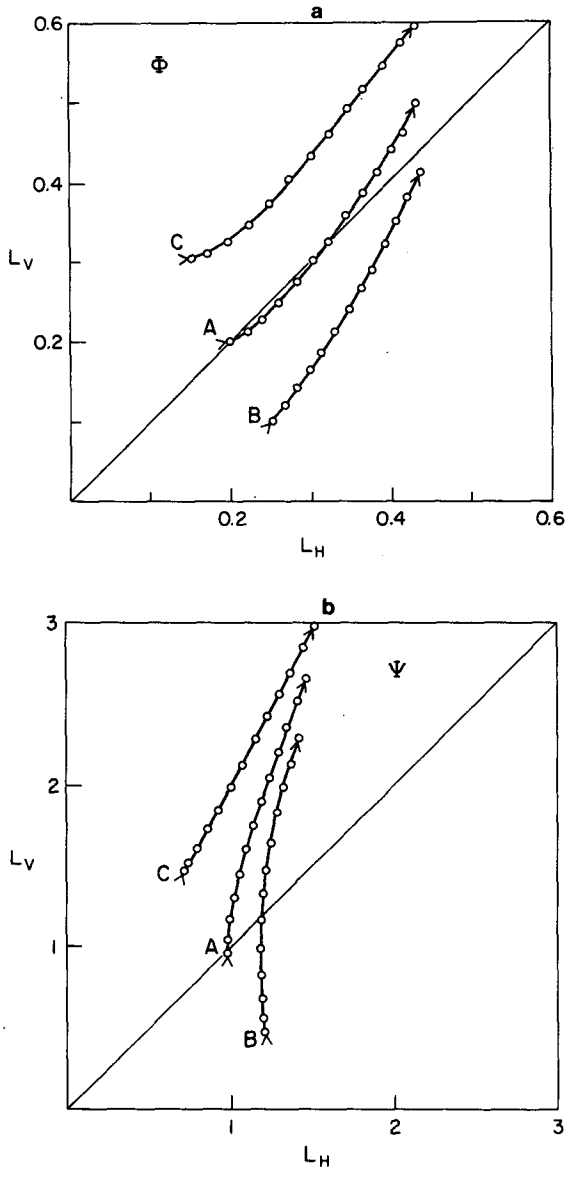

FIG. 4. Evolution of total integral scale length vector, $\mathbf{L} = (L_H, L_V)$ [see Eqs. (2.8a) and (2.8b)]. Streamfunction $\mathbf{L}$ is shown in (a) and vorticity based $\mathbf{L}$ in (b). Labels a, b and c pertain to the three initial conditions (3.2a), (3.2b) and (3.2c).

When we turn from thermal equilibrium to dissipative flows, we encounter dynamical reasons for a near two-dimensionality of large scales, which have nothing to do with considerations involving the Rossby radius or other geometrical considerations. Thus our correlation length scales are intrinsic to the initial spectrum only. If small-scale turbulence

were to be introduced in a layer, we would predict that vertical correlation lengths would tend to grow more rapidly than the normal shift toward large scales, and a virtual large-scale, two-dimensional flow would be reached even if there were no boundaries. Once the vertical length scale exceeds the depth of the fluid, vertical degrees of motion would be progressively eliminated, but the small scales would persist in their three-dimensionality.

The present work is closely related to the two-layer study by Salmon (1978), who considered a two-layer model whose energy spectra are equal, a condition roughly approximating the homogeneity of the present study. Salmon developed the view—using the statistical closures as well as numerical simulations—that the dynamics tend to isotropize the energy among the available wavenumbers, $\mathbf{K}$, $\mathbf{K} \pm k_0$. More precisely, he decomposed the motion into barotropic and baroclinic modes—a decomposition roughly equivalent to the present into kinetic and potential energy except, of course, for the differences in wavenumber representation. Denoting the baroclinic modal energy by $E(K)$ and the barotropic by $U(K)$, Salmon observed that for thermal equilibrium, $E[(K^2 + K_R^2)^{1/2}] = U(K)$, where K_R is the Rossby radius of deformation. In the present study, $K_R = 0$, but a similar shifted spectrum hypothesis, *viz.*, $P(ak) = a^{-3}U(k)$, where $P(k)$ is the potential energy spectrum and $a = 5^{-1/7}$, does account roughly for the shape of the self-similar spectrum found here.

Acknowledgments. This work was undertaken while the author was the Green Scholar at I.G.P.P., Scripps Institution of Oceanography, University of California at San Diego. I am grateful for the opportunity this visit afforded, particularly for numerous discussions with Dr. Rick Salmon. I have also benefited from discussions with Drs. J. Charney, G. Holloway, J. McWilliams, P. Rhines and J. Tribbia. I also wish to thank R. Sadourny for pointing out several errors in an earlier version of the manuscript.

APPENDIX

Derivation of Equations of Motion for $U_n(k)$

Here we give the steps that lead to Eqs. (2.9)–(2.13), the angular harmonic expansions for the equations of motion for the modal total energy spectrum $U(\mathbf{k},t) \equiv k^{-2}\phi(\mathbf{k},t)$. We start by introducing the wavenumber decomposition of (2.1), i.e.,

$$-\nabla^2\psi \equiv \zeta(\mathbf{x},t) = \sum_{\mathbf{k}} \exp(i\mathbf{k}\cdot\mathbf{x})\zeta_{\mathbf{k}}(t), \quad \text{(A1)}$$

$$\dot{\zeta}_{\mathbf{k}}(t) = \sum_{\mathbf{k}=\mathbf{p}+\mathbf{q}} E_{\mathbf{kpq}}\zeta_{\mathbf{p}}\zeta_{\mathbf{q}}, \quad \text{(A2)}$$

TABLE 1. Geometrical coefficients for TFM.

nml	a_{nml}	b_{nml}
000	1	1
002	$-1/5$	$-1/5$
020	$-1/5$	$-1/5$
022	$(1 + 9x^2)/70$	$(1 + 9y^2)/70$
200	-1	-1
202	$(1 + 9y^2)/14$	$(1 + 9y^2)/14$
220	$(1 + 9z^2)/14$	$5/7$
222	$-1/7$	$-1/7$

where

$$E_{\mathbf{kpq}} = (i/2)(p^{-2} - q^{-2})(\mathbf{p} \times \mathbf{q})\cdot\mathbf{n}$$

and $\mathbf{n}$ is a vertical unit vector. Notice that (A2) is formally the same as for two-dimensional turbulence, but $(\mathbf{k},\mathbf{p},\mathbf{q})$ are three- rather than two-dimensional vectors. The eddy-damped Markovian equations for $\dot{U}(\mathbf{k},t)$ are

$$\dot{U}(\mathbf{k},t) = \int \tilde{B}(\mathbf{k},\mathbf{p},\mathbf{q})d\mathbf{p}[U(\mathbf{p})U(\mathbf{q}) - U(\mathbf{k})U(\mathbf{q})]\Theta_{kpq}, \quad \text{(A3)}$$

where

$$d\mathbf{p} = p^2 dp\, \sin\theta_p d\theta_p d\phi_p,$$

$$\mathbf{q} = \mathbf{k} - \mathbf{p},$$

$$\tilde{B}(\mathbf{k},\mathbf{p},\mathbf{q}) = 2(kpq\, \sin\theta\, \sin\phi_p\, \sin\gamma)^2 \times (p^{-2} - q^{-2})(k^{-2} - q^{-2}).$$

Here, θ is the $\mathbf{k}$ polar angle, with respect to $\mathbf{n}$, and the polar axis of $\mathbf{p}$ is chosen to be $\mathbf{k}$, with ϕ_p the azimuthal $\mathbf{p}$ angle. γ is the interior angle between $\mathbf{k}$ and $\mathbf{p}$. We now assume that $U(\mathbf{k})$ is axisymmetric. Then to effect the $d\mathbf{p} = p^2 dp\, \sin\theta_p d\theta_p d\phi_p$ integral in (A3) we need only $(\mathbf{n}\cdot\mathbf{p})/p \equiv \mu_p$ and $(\mathbf{n}\cdot\mathbf{q})/q \equiv \mu_q$. These are

$$\mu_p = \cos\gamma\, \cos\theta - \cos\phi_p\, \sin\gamma\, \sin\theta,$$

$$\mu_q = \cos\beta\, \cos\theta + \cos\phi_p\, \sin\beta\, \sin\theta.$$

We have taken $\mathbf{k}$ in the $(x - z)$ plane and assumed that $\phi = 0$ occurs for the triangle (k,p,q) in the $(x - z)$ plane. These restrictions are valid in view of the assumed axisymmetry. It remains to introduce the spherical harmonic expansion (2.6) into (A3) and to effect the integrals. The result may be written in the form

$$\dot{U}_n(k,t) = \sum_{m,l} \int_\Delta dpdqB(k,p,q)[a_{nml}U_m(p)U_l(q) - b_{nml}U_m(k)U_l(q)]. \quad \text{(A4)}$$

The coefficients a_{nml} and b_{nml} are appropriately weighted integrals of the P_n's and are listed for the

first few (n,m,l) in Table 1. B_{kpq} is given by (2.14). In going from (A3) to (A4), we have eliminated θ_p in favor of $q \equiv |\mathbf{k} - \mathbf{p}|$.

REFERENCES

Carnavale, G., U. Frisch and R. Salmon, 1980: *H*-theorems in fluid dynamics. To be submitted to *J. Phys. A.*

Charney, J. G., 1971: Geostrophic turbulence. *J. Atmos. Sci.*, **28**, 1087–1095.

Herring, J. R., 1975: Theory of two-dimensional anisotropic turbulence. *J. Atmos. Sci.*, **32**, 2254–2271.

——, S. A. Orszag, R. H. Kraichnan and D. G. Fox, 1974: Decay of two-dimensional homogeneous turbulence. *J. Fluid Mech.*, **66**, 417–444.

Jacobs, S. J., and A. Wiin-Nielsen, 1966: On the stability of barotropic basic flow in a stratified atmosphere. *J. Atmos. Sci.*, **23**, 682–687.

Kraichnan, R. H., 1967: Inertial-range in two-dimensional turbulence. *J. Fluid Mech.*, **47**, 525–535.

——, 1971: An almost-Markovian Galilean-invariant turbulence model. *J. Fluid Mech.*, **47**, 513–524.

——, 1976: Eddy viscosity in two and three dimensions. *J. Atmos. Sci.*, **33**, 1521–1536.

——, and J. R. Herring, 1978: A strain based Lagrangian-history turbulence theory. *J. Fluid Mech.*, **88**, 355–367.

Lesieur, M., and D. Schertzer, 1978: Dynamique des gros tourbillons et décroissance de l'énergie cinétique en turbulence tridimensionelle isotrope à grand nombre de Reynolds. *J. Mech.*, **17**, 607–646.

Orszag, S. A., 1974: *Statistical Theory of Turbulence: Les Houches Summer School on Physics.* Gordon and Breach, 216 pp.

Pouquet, A., M. Lesieur and J. C. André, 1975: High Reynolds number simulation of two-dimensional turbulence using a stochastic model. *J. Fluid Mech.*, **72**, 305–319.

Rhines, P. B., 1977: The dynamics of unsteady currents. *The Sea,* Vol. 6, Wiley 189–318.

——, 1979: Geostrophic turbulence. *Annual Review of Fluid Mechanics,* Vol. 11, Annual Reviews, Inc., 401–441.

Salmon, R., 1978: Two-layer quasi-geostrophic turbulence in a simple case. *Geophys. Astrophys. Fluid Dyn.*, **10**, 25–51.

——, G. Holloway and M. C. Hendershott, 1976: The equilibrium statistical mechanics of simple quasi-geostrophic models. *J. Fluid Mech.*, **75**, 691–703.